Mapping brain state-dependent sensory responses across the mouse cortex

Elena Montagni, Francesco Resta, Núria Tort-Colet, Alessandro Scaglione, Giacomo Mazzamuto, Alain Destexhe, Francesco Saverio Pavone, Anna Letizia Allegra Mascaro

iScience

CellPress
OPEN ACCESS

Article

Mapping brain state-dependent sensory responses across the mouse cortex

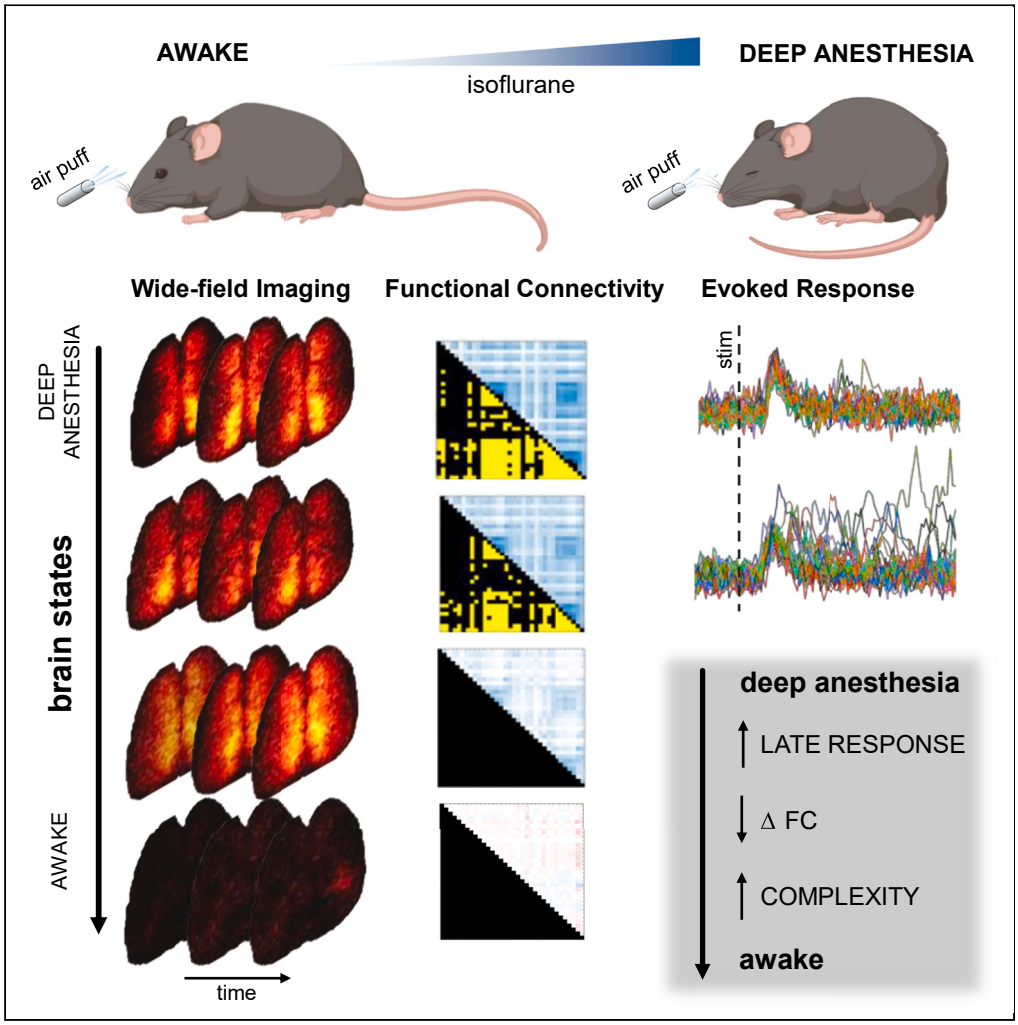

Elena Montagni, Francesco Resta, Núria Tort-Colet, ..., Alain Destexhe, Francesco Saverio Pavone, Anna Letizia Allegra Mascaro

montagni@lens.unifi.it (E.M.)
allegra@lens.unifi.it (A.L.A.M.)

Highlights

The brain state finely tunes sensory-evoked responses across cortical regions

Reducing anesthesia strenghtens the connectivity of the sensory-evoked cortical network

Progressive reduction in response complexity with increasing anesthesia level

Emergence of a late response following slight modulation of the anesthesia level

Montagni et al., iScience 27, 109692
May 17, 2024
https://doi.org/10.1016/j.isci.2024.109692

iScience

CellPress
OPEN ACCESS

Article

Mapping brain state-dependent sensory responses across the mouse cortex

Elena Montagni,[1,2,8,*] Francesco Resta,[1,3,8] Núria Tort-Colet,[4,6,7] Alessandro Scaglione,[1,5] Giacomo Mazzamuto,[1,3,5] Alain Destexhe,[4] Francesco Saverio Pavone,[1,3,5] and Anna Letizia Allegra Mascaro[1,2,5,9,*]

SUMMARY

Sensory information must be integrated across a distributed brain network for stimulus processing and perception. Recent studies have revealed specific spatiotemporal patterns of cortical activation for the early and late components of sensory-evoked responses, which are associated with stimulus features and perception, respectively. Here, we investigated how the brain state influences the sensory-evoked activation across the mouse cortex. We utilized isoflurane to modulate the brain state and conducted wide-field calcium imaging of Thy1-GCaMP6f mice to monitor distributed activation evoked by multi-whisker stimulation. Our findings reveal that the level of anesthesia strongly shapes the spatiotemporal features and the functional connectivity of the sensory-activated network. As anesthesia levels decrease, we observe increasingly complex responses, accompanied by the emergence of the late component within the sensory-evoked response. The persistence of the late component under anesthesia raises new questions regarding the potential existence of perception during unconscious states.

INTRODUCTION

Sensory information needs to be broadcasted among distributed brain areas to be integrated and used to control behavior.[1–3] Since the pioneering work from the Petersen's group, showing the local propagation of the activity from a single barrel to the entire barrel field,[4] there has been a growing interest in the integration of sensory information beyond the primary responsive area. Indeed, distributed aspects of cortical information processing over the entire dorsal cortex were identified as a central mechanism for perceiving peripheral stimuli. One of the first studies to demonstrate the importance of integration was by Guo and colleagues, who established the necessity of serial information flow from sensory to motor areas for perceptual decision-making.[2] The propagation from sensory regions to the entire dorsal cortex was then explored by several groups using wide-field imaging.[1,5–8] Notably, a strong dependence of the evoked spatiotemporal dynamics on the brain state was demonstrated by comparing wakefulness and anesthesia.[9–12] This is in line with a significant body of evidence positing that anesthesia is primarily linked to the breakdown of long-range projections between cortical areas, leading to the impairment of cortical information integration.[13,14] According to the integrated information theory (IIT), disruption of this large-scale integration process is linked to a reduction in the complexity of the locally evoked cortical response.[15] Nevertheless, studies of the complexity associated with a peripheral stimulus, and how this is modulated by the brain state, are largely missing.

It has been demonstrated that in response to a sensory stimulus, the cortex exhibits an early transient response followed by a late response in both awake and anesthetized states.[1,16–19] While the early component of the sensory response reliably represents the stimulus identity, the late component correlates with the stimulus perception and is independent of stimulus modalities.[16,17] Indeed, blocking the late component by optogenetic inhibition in the primary sensory area impairs the perceptual report.[18] Later studies demonstrated that both the early and late responses are broadcasted across the cortex.[1] Specifically, the spatiotemporal pattern of the late response is different from the early response and can be modulated by experience.[16] Considering the link between delayed responses and sensory perception, one might expect that the former would be diminished in unconscious states, such as during anesthesia. In fact, studies have shown that anesthesia significantly influences responses in the primary sensory area, indicating that both early and late components are affected.[20] However, there is a lack of

[1]European Laboratory for Non-Linear Spectroscopy (LENS), Sesto Fiorentino, Italy
[2]Neuroscience Institute, National Research Council, Pisa, Italy
[3]National Institute of Optics, National Research Council, Sesto Fiorentino, Italy
[4]Paris-Saclay University, CNRS, Institut des Neurosciences (NeuroPSI), Saclay, France
[5]Department of Physics and Astronomy, University of Florence, Sesto Fiorentino, Italy
[6]Barcelonaβ Brain Research Center, Barcelona, Spain
[7]Hospital del Mar Medical Research Institute, Barcelona, Spain
[8]These authors contributed equally
[9]Lead contact
*Correspondence: montagni@lens.unifi.it (E.M.), allegra@lens.unifi.it (A.L.A.M.)
https://doi.org/10.1016/j.isci.2024.109692

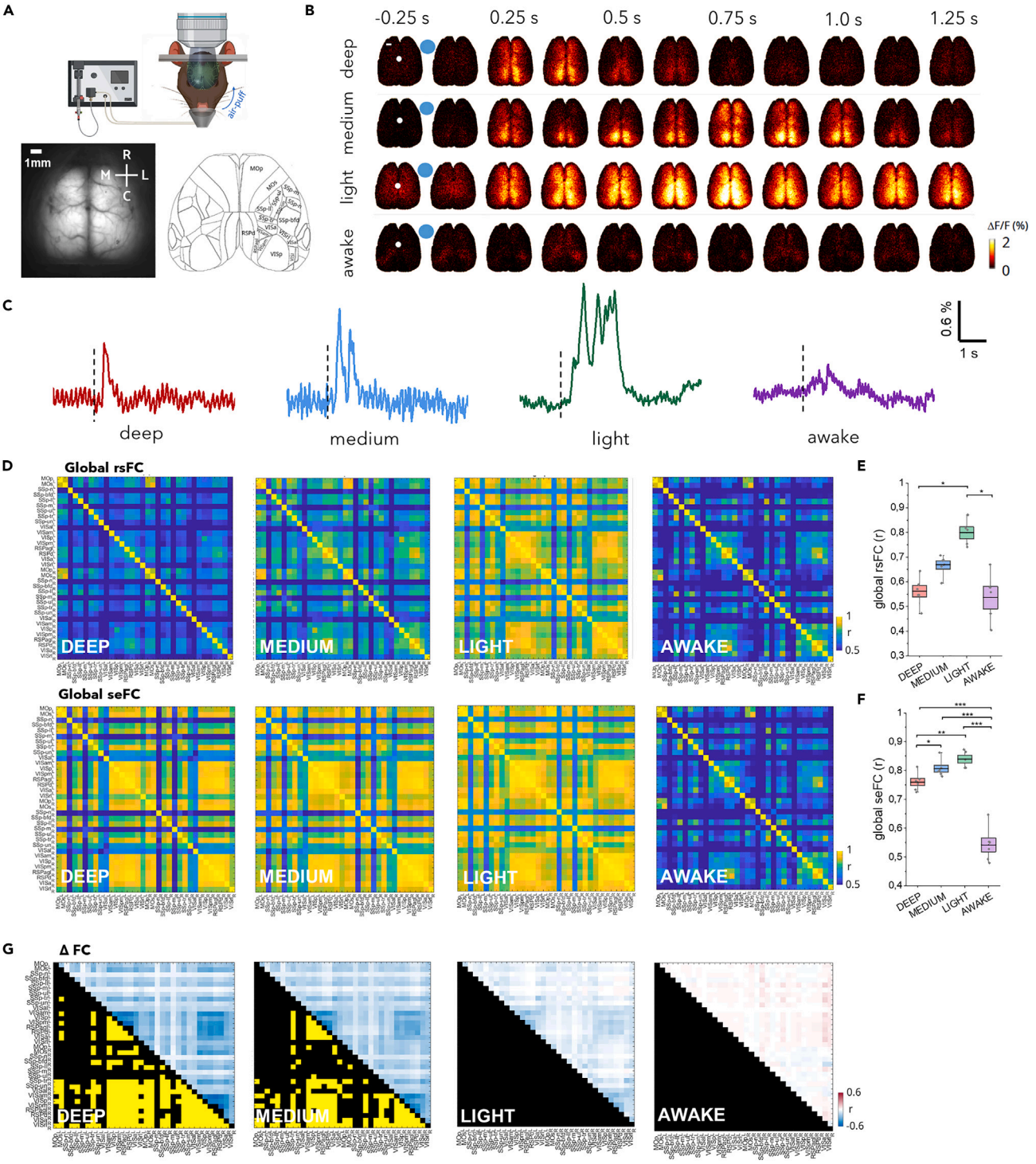

Figure 1. Brain state dependence of the sensory-evoked functional networks

(A) Schematic representation of the whiskers stimulation experiment (upper panel). Averaged raw image of the field of view of the wide-field microscope (lower panel, left, 25 ms exposure time for a duration of 40 s) and Allen Mouse Brain Atlas parcellation (lower panel, right). Scale bar, 1 mm.

(B) Representative image sequences showing the cortical activity in different brain states. White dots represent bregma and blue dots represent the stimulus time. Scale bar, 1 mm.

(C) Single-trial time series showing the cortical response to whisker stimulation in different brain states. The traces represent the average activity of all the pixels in the masked field of view. Vertical dashed lines represent the stimulus time.

Figure 1. *Continued*

(D) Correlation matrices (Pearson's correlation, Fisher's z-transformed) of rsFC in the four brain states from deep anesthesia to wakefulness (top). Sensory-evoked functional connectivity matrices (bottom).

(E) Boxplots displaying the global rsFC calculated averaging the correlation values of all paired cortical regions within animal and brain state. Box shows the standard error range, black line is the mean and whiskers lengths are the extreme data points. LME with Bonferroni correction (awake vs. light $p = 0.01$; deep vs. light $p = 0.02$, $^{*}p < 0.05$). Data are shown as mean ± standard error of the mean (SEM).

(F) Boxplots displaying the global seFC calculated by averaging the correlation values of all paired cortical regions. Box shows the standard error range, black line is the mean and whiskers lengths are the extreme data points. LME with Bonferroni correction (awake vs. deep $p = 1.485e\text{-}07$; awake vs. light $p = 3.260e\text{-}09$; awake vs. medium $p = 2.767e\text{-}08$; deep vs. light $p = 0.002$; deep vs. medium $p = 0.012$) $^{*}p < 0.05$, $^{**}p < 0.01$, $^{***}p < 0.001$) Data are shown as mean ± SEM.

(G) Matrices displaying differences between rsFC and seFC for all the four brain states. The quantification of the differences is shown in the upper part of the matrices and the corresponding statistical significance is reported in the bottom part (black square = non-significant; yellow square = Benjamini-Hochberg corrected $p < 0.05$). $n_{deep} = 6$ mice, $n_{medium} = 6$ mice, $n_{light} = 5$ mice, $n_{awake} = 5$ mice.

understanding on how the early and late responses are modulated by the level of anesthesia across the entire cortex and if there is a threshold for the occurrence of the late response.

In this study, we investigated the brain-state dependence of the large-scale dynamics engaged by multi-whisker stimulation using wide-field calcium imaging of Thy1-GCaMP6f mice. Initially, we examined the connectivity structures within the sensory-activated cortical network across four different brain states: wakefulness and three distinct levels of anesthesia. Then, we delved into how the brain state affects the complexity of the sensory-evoked response and employed a mean-field model to investigate potential mechanisms underlying the experimental findings. Finally, we mapped the spatiotemporal features of the distributed sensory response, both from average and from single trial activity, allowing us to address the long standing question of whether the late response remains observable irrespective of the anesthesia level.

RESULTS

This study aimed to evaluate how the brain state modulates the spatiotemporal integration of the cortical response to sensory stimulation. We investigated sensory-evoked cortical activity in four separate brain states—three anesthesia levels and the awake state. To this end, we performed wide-field calcium imaging of the entire dorsal cortex in transgenic mice expressing GCaMP6f in a subset of excitatory pyramidal neurons (RRID:IMSR_JAX:025393) (Figure 1A). Within this transgenic mouse line, the GCaMP6 signal in the cortical superficial layers primarily originates from the apical tufts of layer 5 neurons and the dendrites and cell bodies of layer 2/3 neurons. This implies that the wide-field signal detected at the cortical surface represents a weighted sum of signals arising mainly from excitatory neurons in these specified layers.

The subjects were either awake or under three levels of anesthesia: deep, medium, and light. The isoflurane concentration was adjusted within the range of 1.3%–1.7% to achieve the desired levels of anesthesia which were cross-validated based on the features of the up and down states extracted from the spontaneous calcium activity traces. The calcium imaging recordings revealed a distributed and asynchronous activation in the awake state and a synchronous and global activation in the light state, which became progressively more localized in medium and deep anesthesia (Figure S1A). Consistent with previous studies,[12,21] all anesthetized states exhibited bistable activity (Figure S1B) with shorter down states and longer up states as the anesthesia decreased (Figures S1C and S1D). Interestingly, the duration of the up-states in light anesthesia is similar to those reported in micro-arousals.[22] The upstate frequency was comparable in light and medium states but dramatically decreased in deep anesthesia (Figure S1E).

Brain state-dependent formation of cortical functional clusters in response to sensory stimulation

Unilateral multi-whisker stimulation elicited a local and transitory response in awake subjects, which was replaced by a persistent and global response across the whole cortex when mice were exposed to a low dose of isoflurane anesthesia (Figures 1B and 1C). Peripheral stimulation in medium and deep anesthesia resulted in a progressively shorter and more localized activation, primarily engaging the medial associative regions (Figure 1B). We initially investigated if the functional connectivity of spontaneous and evoked activity shared similar clusters, and if they were brain-state dependent. Previous studies have reported differences in resting-state functional connectivity (rsFC) between awake and anesthetized states induced by various anesthetic agents,[23] but the correlation structures elicited by sensory stimulation, or sensory-evoked functional connectivity (seFC), are rarely addressed. Within this framework, we examined the brain state dependence of the functional connectivity of excitatory neurons elicited by sensory stimulation and compared it to the resting state. Pearson's correlation (Fisher's z-transformed) was computed between all paired cortical regions and expressed as a matrix for both resting-state (rs) and sensory-evoked (se) conditions per brain state (Figure 1D). Consistent with previous studies,[24] rsFC increased with decreasing anesthesia levels for all cortical pairs, which was reflected in the global rsFC (Figure 1E). Transitioning to the awake state resulted in a drastic decrease in rsFC to levels comparable to deep anesthesia (Figure 1E). Conversely, whisker stimulation increased the seFC of deeper anesthesia levels (Figure 1F) and it is substantially different in wakefulness from all anesthesia levels. Accordingly, the difference matrices highlighted the emergence of a cluster of regions significantly different from the resting state in deep and medium anesthesia. This functional cluster was primarily associated with an increased co-activation of both intra- and inter-hemispheric seFC of posterior regions (Figure 1G). Since in the deep and medium regimes the spontaneous activity is low (as documented by the average duration of the down states, see Figure S1), the distributed increase in cortical activity evoked by the stimulation has a strong impact on the seFC of the network, that significantly separates it from rsFC. Indeed, the differences between the two are strong in the state with lowest spontaneous activity (deep) and are maintained in the medium level. In both regimes, whisker stimulation recruits a sustained activation expanding from the SSbfd to a distributed circuit involving both RSPs and the visual network

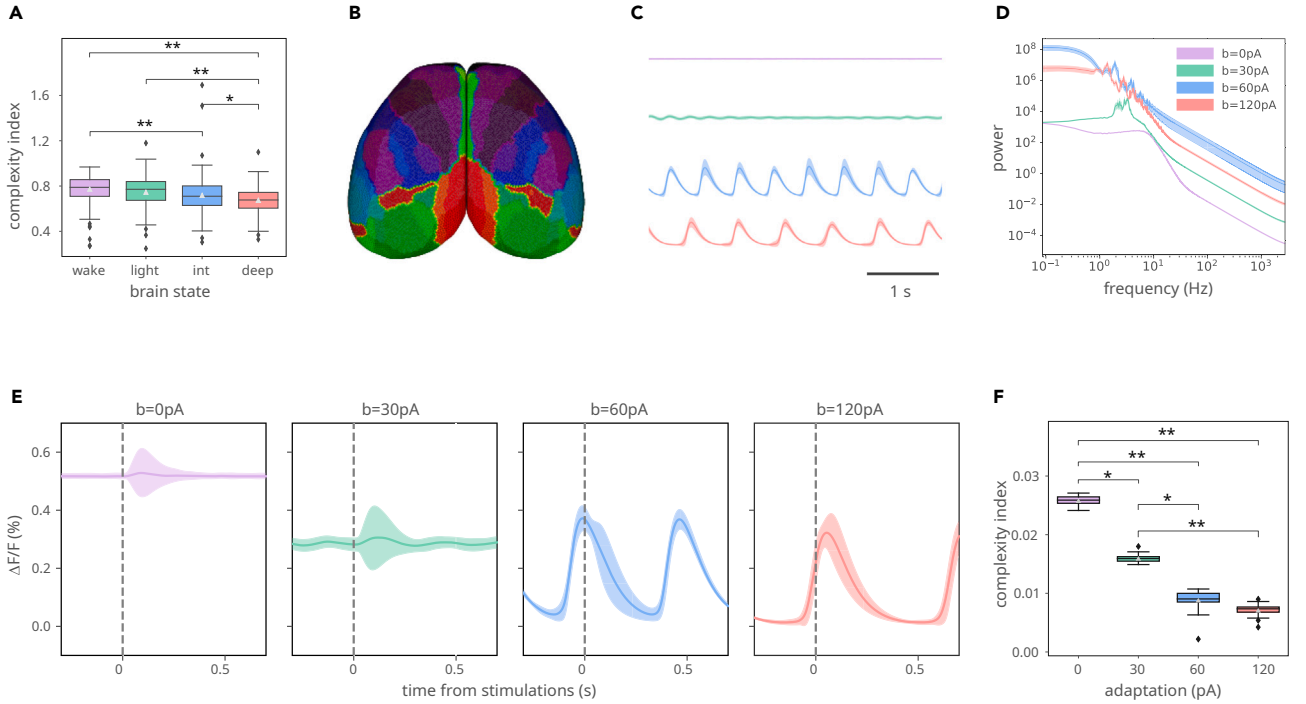

Figure 2. The complexity of the sensory evoked response is brain-state dependent

(A) The Complexity Index (CI) of the sensory-evoked response from wide-field calcium data decreases with increasing levels of anesthesia. Kruskal-Wallis test (H statistic = 70.756, *p* value = 2.94e-15, df = 3) and Dunn's post hoc test with Bonferroni correction. *$p < 0.050$, **$p < 0.001$.

(B) Simulated PCI is calculated from the TVB-Adex model of the entire cortical surface, parcellated according to the Allen Mouse Brain Atlas.

(C) Time course of the modeled calcium signal from asynchronous (top) to slow-wave activity (bottom), as obtained by augmenting the strength of spike-frequency adaptation (b) in the model (0, 30, 60, and 120 pA from top to bottom).

(D) Corresponding power spectra showing the shift toward low frequencies.

(E) Responses to cortical stimulation in different states described in (C).

(F) CI of evoked responses simulated at increasing levels of adaptation. Kruskal-Wallis test (H statistic = 71.002, *p* value = 2.60e-15, df = 3) and Dunn's post hoc test with Bonferroni correction. *$p < 0.050$, **$p < 0.001$. Data are shown as mean ± SEM.

(Figure 1B). The sudden coactivation of this network is arguably mirrored in the high seFC between these regions, both within the stimulated hemisphere and with the homologous counterparts.

Conversely, in light anesthesia and in wakefulness, the high levels of spontaneous activity dictate the correlation levels, which are allegedly less affected by the stimulation. Therefore, rsFC and seFC are not significantly different in these brain states. These results indicate that the connectivity of cortical regions involved in processing incoming sensory information (seFC) significantly diverges from spontaneous activity (rsFC) only under deeper anesthesia.

The complexity of evoked responses decreases with increasing levels of anesthesia

To determine how anesthesia affects the propagation of information across the brain, we computed the complexity index (CI) of the sensory-evoked response from wide-field calcium data and from a computational model. CI was computed for each trial and grouped by brain state condition, using data from all the subjects available for that condition. A Kruskal-Wallis test confirmed that the groups were significantly different (Figure 2A). In fact, the complexity of sensory-evoked activity decreased with increasing levels of anesthesia (Dunn's test with Bonferroni correction, Table S1), consistent with results in humans.[25] Using a whole-brain model of the mouse cerebral cortex (Figure 2B), we simulated different activity states corresponding to asynchronous (wake-like) dynamics (Figure 2C; top trace) and different slow-wave oscillatory states with increasing spike-frequency adaptation to mimic increasing levels of anesthesia (Figure 2C; bottom traces; Figure 2D for power spectra), using a similar procedure as in a previous model of human slow waves. The mouse connectome used here is a parcellation comprising 512 regions. Although it comes with a higher computational cost, it represents a greater spatial resolution compared to previous mouse models implemented in the TVB.[26] All the parameters used to build the mean field models that represent each node of the mouse cortex have been tested against experimental data,[27] and therefore fall in the physiological range. Together, these particularities make this model capable of reproducing the macro scale dynamics observed in the mouse calcium imaging experiments under different levels of anesthesia. In particular, the model is able to show the asynchronous irregular activity observed during wakefulness by setting the strength

of spike-frequency adaptation (b) to zero and a bistable regime (up and down states) when b is sufficiently large. For low values of b, the model still shows an oscillatory regime, although the down states do not become completely silent. The response to cortical stimulation in the model is shown in Figure 2E, in the same asynchronous and slow-wave states. In this figure, lines and shaded areas correspond to the mean and standard deviation over trials of the global evoked response (averaged over areas) to a stimulus applied in the model node (area) corresponding to the right barrel field cortex, time-locked to the stimulus onset. The onset of the stimulus was randomly delayed in each trial, without discarding trials in which it coincided with an up state. Note that, apart from the expected increase of variability at the onset of each up state, there is another source of variability linked to the stimulus response at around 0.2–0.3s from the stimulus onset. The complexity of this response was quantified using CI for each trial and condition. As in the experiments, we found that the CI was significantly different among brain states (Figure 2F; Krisukal-Wallis test) and decreased with the strength of spike-frequency adaptation (Dunn's test with Bonferroni correction, Table S2) showing that the spread of the complexity of the evoked response is diminished in slow-wave states in both model and experiments.

The spatiotemporal features of the sensory information broadcasting among cortical regions depend on the brain state

We hypothesized that the differences in the spatiotemporal features of the evoked response could underlie the modulation of the complexity with the brain state. Consistent with previous studies,[1,6] monolateral whisker stimulation evoked a distributed cortical response with brain state dependency. We analyzed seventeen representative cortical regions per hemisphere to reconstruct topographic response maps based on the mean response (Figure 3A). Interestingly, the stimulated barrel cortex (ss-bfd$_R$) showed stable onset, rising slope, and maximum amplitude across all brain states (Tables S3–S6). Differences however arose in the time to peak, which occurred later in light anesthesia and in the average response duration, longer for medium and light anesthesia (Tables S5–S7).

The integration of the response across the other cortical regions changed significantly depending on the brain state. While the onset latency was uniform across all brain states (Table S3; Figure 3B), the rise slope of the majority of investigated areas was significantly high in deep anesthesia and gradually decreased from medium to the awake state (Table S4; Figure 3C). Conversely, the time to peak was significantly delayed only in light anesthesia compared to all other brain states for most cortical areas examined (Table S5; Figure 3D). Notably, the time to reach the peak displayed regional variability in wakefulness, whereas it was relatively consistent across brain areas under anesthesia (Table S5; Figure 3E). The response peak exhibited higher amplitude in all the three anesthetized states compared to wakefulness (Table S6; Figure 3E). Finally, light and medium anesthesia were both characterized by increased persistence of the response (Table S7; Figure 3F).

These findings highlight the stability of the average response in the primary sensory area ss-bfd$_R$, suggesting that the cortical representation of stimulus features is stable regardless of the brain state. In contrast, the integration of sensory input across the entire dorsal cortex is strongly influenced by the brain state being finely tuned by the anesthesia level.

Slight adjustments to the anesthesia level result in the appearance of the late response to the stimulus

Our results revealed that sensory stimulation engaged a FC cluster that did not differ between medium and deep anesthesia (Figures 1G and S2). This similarity was also observed for the activation in the primary sensory area ss-bfd$_R$ which we found comparable in these two brain states. However, significant brain state-dependent differences were observed in the complexity of the evoked response and in the integration of the response across the entire cortex. One key feature that distinguished deep and medium was the average response duration, which could be linked to an increased likelihood of the emergence of a late component. Therefore, we hypothesized that the late component could be responsible for the increased complexity and duration of the evoked response in medium anesthesia. Specifically, we wondered if the brain state could selectively modulate different aspects of these two time domains.

To test these ideas, we conducted a single trial analysis of the sensory-evoked response in the same animals under deep and medium anesthesia. We analyzed six representative regions per hemisphere: the primary and secondary motor cortices (M1 and M2), primary somatosensory area of the barrel field (SS-bfd), primary somatosensory area of the trunk (SS-tr), primary visual cortex (V1), and retrosplenial cortex (RSP) (Figure 4A; Table S8). The exemplary traces showed that a stereotyped early response was present in both anesthesia levels, followed by a late response that was predominantly observed in medium anesthesia and largely absent in deep anesthesia (Figure 4B). The analysis of the early response revealed that the onset was symmetrical between hemispheres and was not dependent on the anesthesia level (Figure 4C). Interestingly, the time to peak and full width at half maximum (FWHM) were increased in medium compared to deep anesthesia, with a prominent contribution from the contralateral hemisphere to the stimulus (Figures 4D and 4E). Although the peak amplitude of the early component exhibited asymmetry within a single brain state due to higher values in the contralateral hemisphere to the stimulus, it did not significantly differ between the two anesthetized levels indicating that it was not sensitive to the brain state (Figure 4F). Moreover, both the rise and decay slopes were consistently lower on the contralateral hemisphere in most of the analyzed regions and the rising slope also showed higher values in deep compared to medium anesthesia (Figures 4G and 4H). Overall, these features indicate that sensory stimulation leads to a slower and longer early response in medium anesthesia while maintaining the same amplitude as in deep anesthesia.

We previously highlighted the presence of a late component, primarily observed in the medium state. The probability of evoking a late response dramatically decreased from medium to deep anesthesia (Figure 4I). Consequently, in our further analysis, we focused on the comparison between the early and late components within medium anesthesia. The late response reached the maximum peak almost uniformly across brain regions and hemispheres, approximately 500 ms after the early response (Figures 4J and S3A). However, the amplitude of the late response exhibited a precise topographic modulation, with higher values in the contralateral hemisphere, except for BF and RSP (Figures 4K

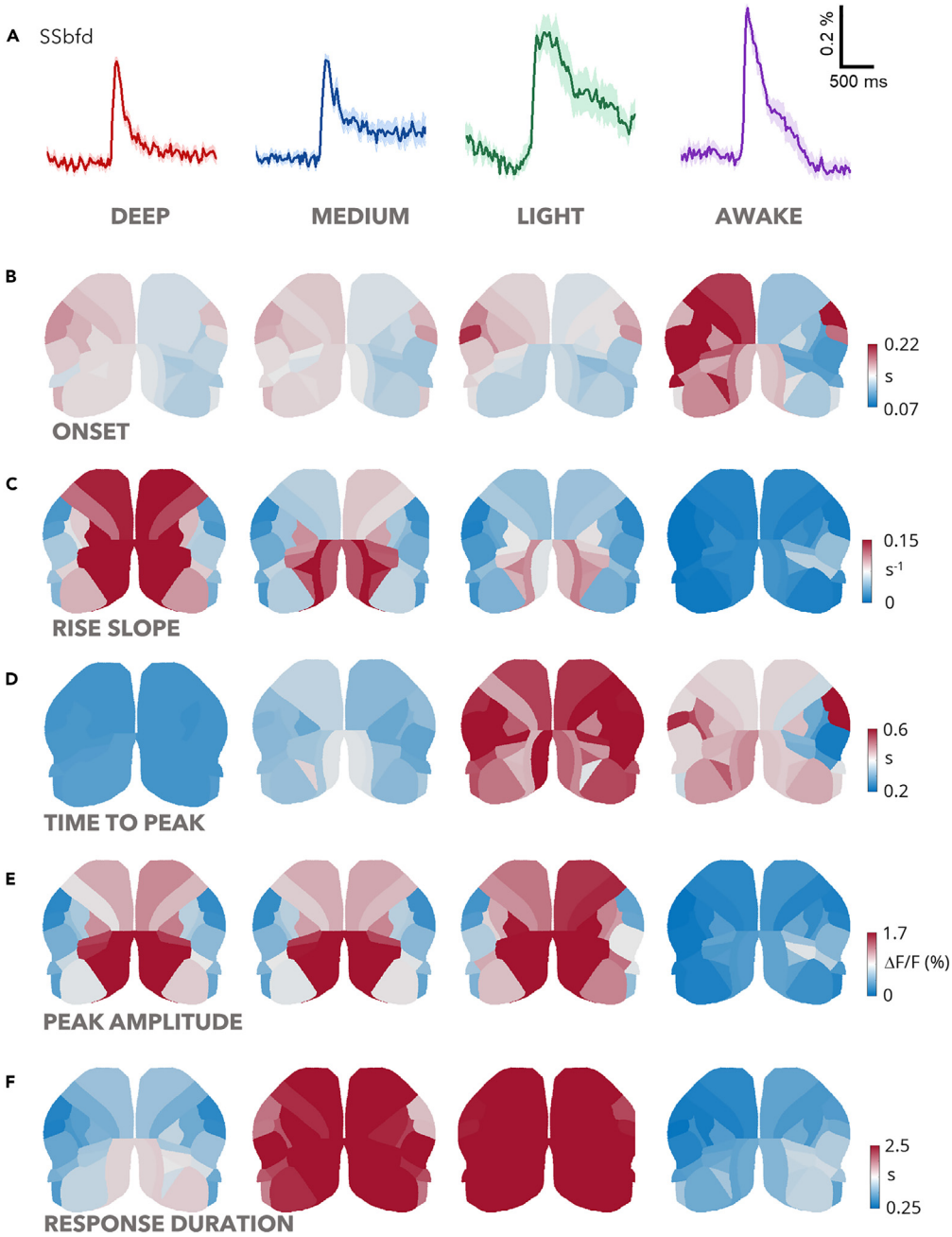

Figure 3. Brain state dependence of the spatiotemporal features of the distributed sensory-evoked response

(A) Average traces showing the sensory-evoked activity in the primary sensory area, SSp-bfd, in awake mice and under increasing levels of isoflurane. Solid lines indicate the mean and the shaded area denote SEM.

(B–F) Cortical maps registered to the Allen Mouse Brain Atlas displaying the quantification of the onset (B), rise slope (C), time to peak (D), peak amplitude (E) and response duration (F), of the sensory-evoked activity. n_{deep} = 6 mice, n_{medium} = 6 mice, n_{light} = 5 mice, n_{awake} = 5 mice.

and S3B). The duration of the early and late activations, measured by FWHM, was mostly comparable across all cortical regions, with a few exceptions (M1 and SSTr) (Figure 4L).

Considering that the late response has been previously linked to the subjective perceptual report of the stimulus,[18] these findings might imply that medium anesthesia, as opposed to deep anesthesia, is associated with heightened integration of the sensory stimulus. Consequently, even minor adjustments to anesthesia levels result in substantial variations in the distributed cortical processing of the stimulus.

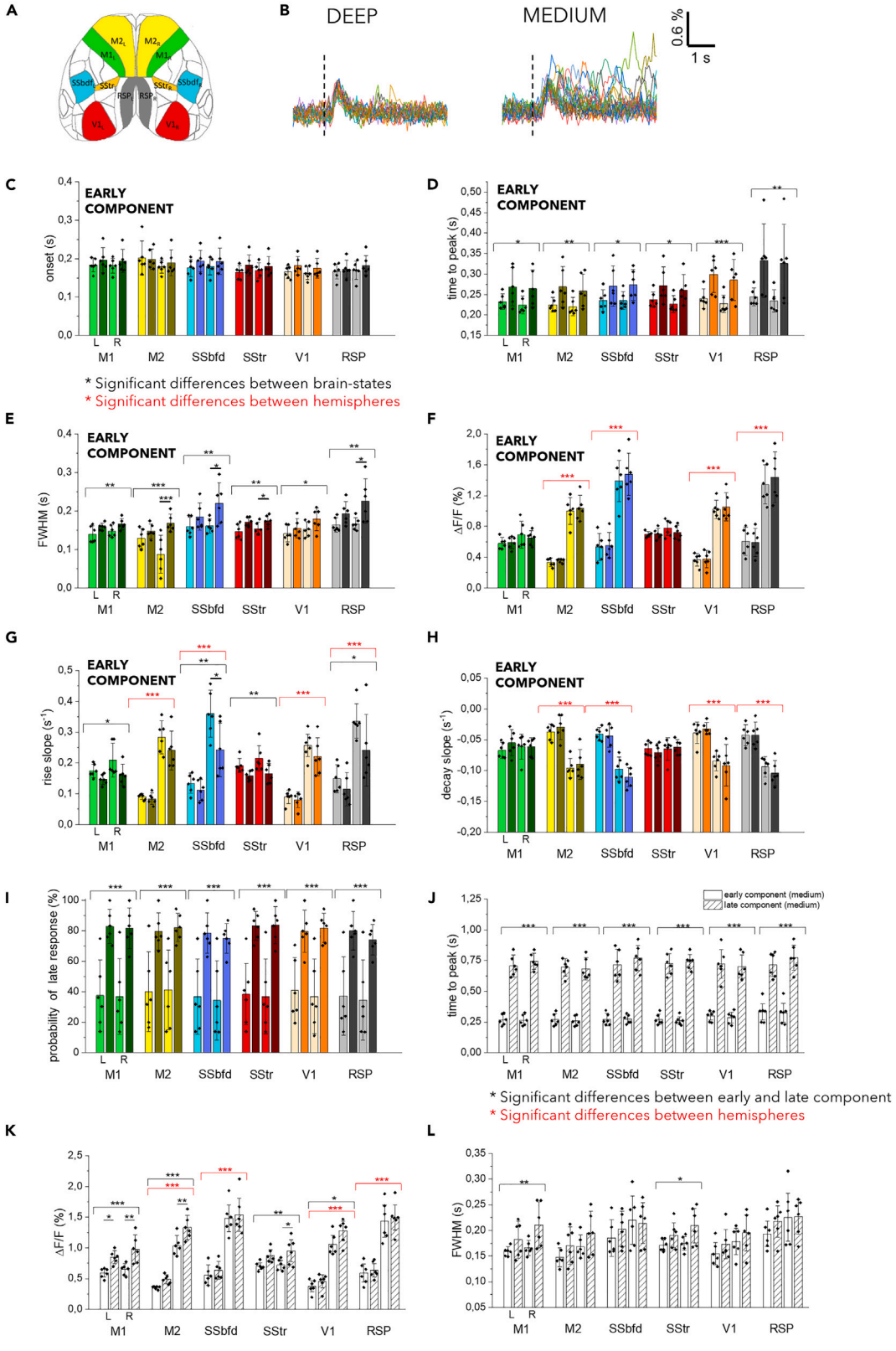
A
B
DEEP
MEDIUM
0.6 %
1 s
C
EARLY COMPONENT
onset (s)
D
time to peak (s)
* Significant differences between brain-states
* Significant differences between hemispheres
E
FWHM (s)
F
ΔF/F (%)
G
rise slope (s⁻¹)
H
decay slope (s⁻¹)
I
probability of late response (%)
J
early component (medium)
late component (medium)
* Significant differences between early and late component
* Significant differences between hemispheres
K
L
M1
M2
SSbfd
SSbfd
SStr
V1
RSP

Figure 4. Small variations in the anesthesia level determine substantial changes in the late component of the sensory-evoked response

(A) Allen Mouse Brain Atlas parcellation used to identify the cortical regions for single-trial analysis (M1, primary motor cortex; M2, Secondary motor cortex; SSbdf, primary somatosensory barrel field cortex; SStr, primary somatosensory cortex trunk; RSP, Retrosplenial cortex; V1, primary visual cortex; L, left; R, right).

(B) Sensory-evoked calcium activity in the Barrel field cortex under deep (on the right) and medium (on the left) anesthesia in the same representative animal (dashed line indicates the timing of the stimulus, *n* stimuli = 11). Column chart showing onset time (C), time to peak (D), FWHM (E), ΔF/F% (F), rise slope (G) and decay slope (H) of the early component for six cortical regions in the left (L) and in the right (R) hemisphere under deep (patterned columns) and medium (empty columns) anesthesia. Whisker length is the standard error.

(I) Boxplot showing the probability of late response for six cortical regions in the left (L) and in the right (R) hemisphere under (patterned columns) and medium (empty columns) anesthesia. Whisker length is the standard error. Boxplot showing comparing time to peak (J), ΔF/F% (k) and FWHM (L) of the early (empty columns) and late component (patterned columns) for six cortical regions in the left (L) and right (R) hemisphere under medium anesthesia. *N* mice = 6. two-way ANOVA with Bonferroni correction (*$p < 0.05$; **$p < 0.01$; ***$p < 0.001$), Data are shown as mean ± SEM.

In conclusion, our observations on the late response suggest that the mechanisms underlying stimulus perception may be activated even under medium levels of anesthesia.

DISCUSSION

Different states of the brain are characterized by alterations in the spatiotemporal pattern of neuronal activity in many brain areas,[11] which can influence responses to incoming sensory information.[9,10] To investigate the interplay of local and distributed cortical responses to sensory stimulation and its dependence on the brain state, we took advantage of wide-field optical imaging of excitatory neurons in Thy1-GCaMP6f mice. We examined the distributed cortical activity evoked by unilateral whisker stimulation across four distinct brain states, including three levels of isoflurane anesthesia and wakefulness.

Our results indicate that increasing levels of anesthesia are associated with (i) the emergence of a cluster of posterior regions exhibiting higher intra- and inter-hemispheric correlation during sensory stimulation (ii) a progressive loss of cortical response complexity (iii) a reduction in the duration of the mean response across all cortical regions, which is arguably due to (iv) the disappearance of a late component of the sensory-evoked response.

Cortical connectivity may reflect distinct patterns of activation in the evoked activity compared to the resting state and could be modulated differently by experience.[28,29] The vast majority of studies comparing resting state and task-evoked FC are based on human fMRI measures.[30–37] They show that the rs- and se-FC can share common patterns, being them generated by the activation of partially overlapping networks. Here we compared the seFC to the rsFC and found significant differences only in deeper anesthesia levels. Our findings, which support the concept that the functional connectivity of sensory-evoked cortical responses can significantly diverge from that of spontaneous activity, provide a crucial insight by indicating that this distinction is significantly influenced by the brain state. Surprisingly, the difference between rsFC and seFC becomes more pronounced in deeper anesthesia states, where one would expect more stereotypical activity regardless of the source of activation (internal vs. peripheral). Conversely, the similarity in the coactivation of the cortical network in the wakefulness state indicates that the main driver is likely the constantly changing patterns of activation, regardless of the origin of the signal.

Anesthesia is well-known to alter rsFC by changing both (i) systemic variables such as temperature,[38] heartbeat frequency, and respiration rate,[39,40] and (ii) neural activity, from brain metabolism to cerebral blood flow (CBF),[38,41] and neurovascular coupling.[42–44] This is a strong limitation for preclinical fMRI-based rsFC, obtained mostly under anesthesia. Indeed, positive correlations have been documented in human subjects between regional CBF and FC in all resting brain networks; Under isoflurane anesthesia, vessel diameter and CBF increase drastically within the first 10 min following induction,[45] but following this initial phase, it stay flat within the ranges of isoflurane concentration used in this work (1–1.5%).[45,46] Therefore, according to this study, the contribution of hemodynamics to the calcium signals in the three anesthesia states should be negligible.

On top of the consequences on the rsFC, an increase in CBF could limit neurovascular reactivity and affect seFC. Another potential mechanism contributing to alterations in the seFC across different levels of anesthesia may be attributed to the ongoing dynamics during sensory stimulation. Previous studies have demonstrated that anesthesia-dependent changes in overall excitability can influence the dynamical interdependencies among elements of the cortical network, thereby affecting both the functional and perturbational complexity of its collective dynamics.[12] Consistent with this framework, our results indicate decreasing complexity values with increasing levels of anesthesia, possibly arising from changes in the dynamic relationships between cortical regions. This suggests a plausible mechanism underlying the alterations in seFC under varying levels of anesthesia. Future research is needed to further investigate how sensory experience can modify seFC and how this process is dependent on the level of anesthesia.

The quantification of the complexity of the evoked response in the different brain states was done using CI, which was found to globally decrease with the depth of anesthesia (Figure 2A). This global decrease could be replicated by a mouse whole-brain model, where the perturbational complexity index (PCI) was inversely proportional to the level of adaptation (Figure 2F). This result must be put in perspective with findings in humans, where the evoked activity is maximally complex in the awake state,[47] and drops to low values during sleep or anesthesia.[25] This result was also replicated by a whole-brain model.[48,49] It must be noted, however, that in the present work, a sensory input was used, while the model has been developed to simulate direct cortical stimulation.[5] This may explain why the PCI variations are larger in the model compared to the experiments, a point that should be checked when more precise models are available to simulate sensory inputs.

PCI was previously established as a tool to define the (un)consciousness level in patients.[25] Here we measured the complexity of the cortical response evoked by sensory stimulation instead of transcranial magnetic stimulation (TMS); however, our results confirm a reduction

of the complexity with increasing levels of anesthesia. This is an encouraging premise for future studies comparing sensory- and TMS-evoked responses, to test if specific sensory-stimulation protocols could be employed in the place of TMS (which is more expensive in terms of personnel and instrumentation). To this aim, further experiments shall perform a rigorous comparison with the TMS-EEG benchmark. Specifically, future investigations shall explore what is the TMS-EEG correlation of our late response. However, we recognize that a comparison of the late response between the two measures can be difficult due to the presence of the peripheral feedback, which only pertains to the sensory-evoked activations and is modulated by the anesthesia level.

A similar approach based on sensory stimulation was recently proposed to assess consciousness in infants.[50] As they point out, peripherally evoked activity requires an intact thalamocortical system, which could not be the case for some unconscious patients.

In studies investigating the neuronal correlates of sensory stimuli, averaging signals across trials is a common approach to enhance the signal-to-noise ratio and reveal the underlying neural response. However, this averaging approach may mask meaningful time-varying neural fluctuations that can be important for understanding brain function.[3,51] Furthermore, it has been demonstrated that the trial-to-trial variability of sensory-evoked responses is dependent on the cortical state.[9,52,53] To overcome these limitations, we utilized the high signal-to-noise ratio and fast dynamics of the GCaMP6f indicator in combination with the temporal resolution of our optical setup to explore the sensory-evoked dynamics at the single-trial level. Nevertheless, it should be noted that boundaries separating two regions may contain information from both, given the spatial resolution of the recording system. This could increase the correlation values. We therefore limited our single trial analysis to a few, spatially separated, cortical areas. This allowed us to characterize the brain-state dependence of the late response to sensory stimulation and uncover specific features of the early and late components that are hard to disentangle from the average response.

The impact of brain state on the coding of a stimulus has mainly been investigated at the local level, particularly in the primary sensory area.[9,16] These studies primarily focus on the temporal organization of locally evoked activity during anesthesia and analyze complexity, onset, and duration, with findings comparable to our observations for the medium anesthesia level.[16]

In the primary sensory area (SSbfd contralateral to the stimulus), our results demonstrate that the average response is stable in terms of amplitude, onset, and rise time across all brain states. Nonetheless, in other cortical regions, most of the spatiotemporal features are markedly influenced by the brain state. This suggests that it is predominantly the late processing and its broadcasting throughout the dorsal cortex that are dependent on the brain state, as demonstrated by the significant appearance of a late response only beyond a certain threshold of isoflurane level. This phenomenon could be attributed to the distributed nature of the late response. Specifically, in medium compared to deep anesthesia, we observed a subtle increase in the PCI, indicative of more complex inter-area interactions that may lead to a time-varying second peak. Additionally, in this state, there is an increase in the upstate's frequency, suggesting heightened dynamic activities that could contribute to the variability observed in the late response.

These findings align with previous work suggesting that the organization of the early late component in sensory-evoked activity can be modulated by the brain state.[16,54] We observed that the early component of the evoked response exhibits a longer time to peak and duration (FWHM) across all cortical regions in medium anesthesia compared to deep anesthesia (Figures 4D and 4E). Additionally, the early component shows strong asymmetry in M2, SSbfd, and RSP but similarities between brain states in terms of amplitude (Figure 4F), indicating differences in the perception of stimulus features between hemispheres but no influence of the anesthesia level on amplitude. In contrast, the late component is strongly brain-state dependent, as the probability of evoking a late response dramatically drops in deep anesthesia (Figure 4I). Previous studies have demonstrated that the late activity phase is critical for perception, as silencing or blocking it interferes with stimulus perception or detection.[17,18,55] Therefore, our results suggest that the perception of the stimulus could still be present under anesthesia and can disappear only at very deep anesthesia levels.

It has been suggested that stimulus perception requires the recirculation of activity through recurrent local and horizontal connections, which typically influences the late phase of the response.[17] Recent studies have indicated that neurons in higher areas are responsible for sending cortical feedback, which is reflected in the late response in the primary sensory area.[56–58] Our findings show that the late response exhibits a greater delay in SSbfd and RSP compared to M2 in the contralateral hemisphere to the stimulus, suggesting an anteroposterior sequence of activation starting from neurons in the secondary motor cortex and later reaching the primary sensory region. The high amplitude of the late component in SSbfd and RSP, followed by M2 and V1, indicates their substantial involvement in cortico-cortical feedback. Given that the late response's amplitude and activity recirculation are both related to stimulus perception, our results support the hypothesis that stimulus perception is a distributed process involving multiple cortical areas beyond the directly stimulated one (Figures S2 and S4), with specific involvement of M2, SSbfd, and RSP in the late response. These results demonstrate that the majority of features of sensory-evoked activity that are sensitive to the brain state belong to the late component of the cortical response. The perception of the stimulus is strongly influenced by the complexity of the brain state and likely depends not only on the local manifestation of a late response but also on how this response is propagated and integrated by other cortical regions.

In conclusion, our study highlighted the presence of a late component in deeper anesthesia, which is highly relevant for consciousness studies and to define clear biomarkers of external awareness in anesthetized patients.

Limitations of the study

In this study, the GCaMP indicator is expressed in excitatory neurons in both superficial (L2/3) and deep (L5) cortical layers. Moreover, the wide-field calcium signal is a population summation of the neuronal activity that includes soma, dendrites, and axons in a volume beneath

the surface.[59] This combined approach limits our capability to distinguish between cortical layers and the associated cortical hierarchies which shape the communications between regions.[60]

Moreover, activity propagation in the cortex occurs at the spikes timescale in the order of a few milliseconds. One limitation of wide-field imaging of Thy1-GCaMP6f mice is the temporal resolution that is mainly limited by the indicator decay kinetics for single action potential, which is in the range of hundreds of milliseconds.[61,62] The limited temporal resolution potentially masks fast events and restricts the investigation to the lower part of the frequency spectrum.

In this study, we focused on the differences between decreasing levels of anesthesia and wakefulness, considering the awake state as a unique brain state. However, it has been reported that during wakefulness, a subject explores distinct behavioral states such as quiet vs. alert or the level of task engagement. Importantly, the behavioral state has been demonstrated to affect the coding of sensory stimuli in the somatosensory cortex.[63,64] Therefore, considering the awake state as a single brain state limits our capability to explain the variability of the cortical response at the single trial level.

STAR★METHODS

Detailed methods are provided in the online version of this paper and include the following:

- KEY RESOURCES TABLE
- RESOURCE AVAILABILITY
  - Lead contact
  - Materials availability
  - Data and code availability
- EXPERIMENTAL MODEL AND STUDY PARTICIPANT DETAILS
- METHOD DETAILS
  - Intact-skull preparation
  - Imaging setup
  - Awake imaging
  - Anesthetized imaging
  - Whisker stimulation
  - Computational model
  - Data analysis
  - Functional connectivity and network analyses
  - Quantitative analysis of perturbed activity
  - CI analysis
- QUANTIFICATION AND STATISTICAL ANALYSIS

SUPPLEMENTAL INFORMATION

Supplemental information can be found online at https://doi.org/10.1016/j.isci.2024.109692.

ACKNOWLEDGMENTS

This work has been funded by the European Community (Human Brain Project, H2020–785907 and H2020-945539). In addition, this project has been supported by the Italian Ministry for Universities and Research, project THE Tuscany Health Ecosystem ECS_00000017 MUR_PNRR, and in the framework of Eurobioimaging (ESFRI research infrastructure) - Advanced Light Microscopy Italian Node. The study was supported by the European Union's Horizon 2020 Framework Programme for Research and Innovation under grant agreement no. 654148 Laserlab-Europe.

We also thank Dr. Giuseppe De Vito for support on statistical analysis. We thank the Centre National de la Recherche Scientifique (CNRS) for financial and technical support.

AUTHOR CONTRIBUTIONS

A.L.A.M., A.D., and F.S.P. conceived the study; E.M. and F.R. did the experiments; E.M. analyzed experimental data; A.S. helped in developing the analysis tools; G.M. developed the software for the imaging setup; N.T.C. participated in the analysis and realized the computational model; F.S.P. contributed funding and resources. E.M., F.R., N.T.C., A.D., A.L.A.M. discussed the results and participated to write the paper; A.L.A.M. and A.D. co-supervised the study.

DECLARATION OF INTERESTS

The authors declare no competing interests.

Received: November 2, 2023
Revised: February 20, 2024
Accepted: April 5, 2024
Published: April 9, 2024

REFERENCES

1. Song, C., Piscopo, D.M., Niell, C.M., and Knöpfel, T. (2018). Cortical signatures of wakeful somatosensory processing. Sci. Rep. *8*, 11977.
2. Guo, Z.V., Li, N., Huber, D., Ophir, E., Gutnisky, D., Ting, J.T., Feng, G., and Svoboda, K. (2014). Flow of cortical activity underlying a tactile decision in mice. Neuron *81*, 179–194.
3. Liu, M., Liang, Y., Song, C., Knöpfel, T., and Zhou, C. (2022). Cortex-wide spontaneous activity non-linearly steers propagating sensory-evoked activity in awake mice. Cell Rep. *41*, 111740.
4. Ferezou, I., Bolea, S., and Petersen, C.C.H. (2006). Visualizing the cortical representation of whisker touch: voltage-sensitive dye imaging in freely moving mice. Neuron *50*, 617–629.
5. Mohajerani, M.H., Chan, A.W., Mohsenvand, M., LeDue, J., Liu, R., McVea, D.A., Boyd, J.D., Wang, Y.T., Reimers, M., and Murphy, T.H. (2013). Spontaneous cortical activity alternates between motifs defined by regional axonal projections. Nat. Neurosci. *16*, 1426–1435.
6. Rosenthal, Z.P., Raut, R.V., Bowen, R.M., Snyder, A.Z., Culver, J.P., Raichle, M.E., and Lee, J.M. (2021). Peripheral sensory stimulation elicits global slow waves by recruiting somatosensory cortex bilaterally. Proc. Natl. Acad. Sci. USA *118*, e2021252118.
7. Motaharinia, M., Gerrow, K., Boghozian, R., White, E., Choi, S.E., Delaney, K.R., and Brown, C.E. (2021). Longitudinal functional imaging of VIP interneurons reveals sup-population specific effects of stroke that are rescued with chemogenetic therapy. Nat. Commun. *12*, 6112.
8. Padawer-Curry, J.A., Bowen, R.M., Jarang, A., Wang, X., Lee, J.M., and Bauer, A.Q. (2023). Wide-Field Optical Imaging in Mouse Models of Ischemic Stroke. Methods Mol. Biol. *2616*, 113–151.
9. Pachitariu, M., Lyamzin, D.R., Sahani, M., and Lesica, N.A. (2015). State-dependent population coding in primary auditory cortex. J. Neurosci. *35*, 2058–2073.
10. Schwalm, M., Schmid, F., Wachsmuth, L., Backhaus, H., Kronfeld, A., Aedo Jury, F., Prouvot, P.H., Fois, C., Albers, F., van Alst, T., et al. (2017). Cortex-wide BOLD fMRI activity reflects locally-recorded slow oscillation-associated calcium waves. Elife *6*, e27602.
11. Pais-Roldán, P., Takahashi, K., Sobczak, F., Chen, Y., Zhao, X., Zeng, H., Jiang, Y., and Yu, X. (2020). Indexing brain state-dependent pupil dynamics with simultaneous fMRI and optical fiber calcium recording. Proc. Natl. Acad. Sci. USA *117*, 6875–6882.
12. Dasilva, M., Camassa, A., Navarro-Guzman, A., Pazienti, A., Perez-Mendez, L., Zamora-López, G., Mattia, M., and Sanchez-Vives, M.V. (2021). Modulation of cortical slow oscillations and complexity across anesthesia levels. Neuroimage *224*, 117415.
13. Alkire, M.T., Hudetz, A.G., and Tononi, G. (2008). Consciousness and anesthesia. Science *322*, 876–880.
14. Redinbaugh, M.J., Phillips, J.M., Kambi, N.A., Mohanta, S., Andryk, S., Dooley, G.L., Afrasiabi, M., Raz, A., and Saalmann, Y.B. (2020). Thalamus Modulates Consciousness via Layer-Specific Control of Cortex. Neuron *106*, 66–75.e12.
15. Sarasso, S., Rosanova, M., Casali, A.G., Casarotto, S., Fecchio, M., Boly, M., Gosseries, O., Tononi, G., Laureys, S., and Massimini, M. (2014). Quantifying cortical EEG responses to TMS in (un)consciousness. Clin. EEG Neurosci. *45*, 40–49.
16. Bermudez-Contreras, E., Schjetnan, A.G.-P., Luczak, A., and Mohajerani, M.H. (2023). Sensory experience selectively reorganizes the late component of evoked responses. Cereb. Cortex *33*, 2626–2640.
17. Kirchberger, L., Mukherjee, S., Schnabel, U.H., van Beest, E.H., Barsegyan, A., Levelt, C.N., Heimel, J.A., Lorteije, J.A.M., van der Togt, C., Self, M.W., and Roelfsema, P.R. (2021). The essential role of recurrent processing for figure-ground perception in mice. Sci. Adv. *7*, eabe1833.
18. Sachidhanandam, S., Sreenivasan, V., Kyriakatos, A., Kremer, Y., and Petersen, C.C.H. (2013). Membrane potential correlates of sensory perception in mouse barrel cortex. Nat. Neurosci. *16*, 1671–1677.
19. Dehaene, S., and Changeux, J.-P. (2011). Experimental and theoretical approaches to conscious processing. Neuron *70*, 200–227.
20. Lee, H., Tanabe, S., Wang, S., and Hudetz, A.G. (2021). Differential Effect of Anesthesia on Visual Cortex Neurons with Diverse Population Coupling. Neuroscience *458*, 108–119.
21. Torao-Angosto, M., Manasanch, A., Mattia, M., and Sanchez-Vives, M.V. (2021). Up and Down States During Slow Oscillations in Slow-Wave Sleep and Different Levels of Anesthesia. Front. Syst. Neurosci. *15*, 609645.
22. Tort-Colet, N., Capone, C., Sanchez-Vives, M.V., and Mattia, M. (2021). Attractor competition enriches cortical dynamics during awakening from anesthesia. Cell Rep. *35*, 109270.
23. Aedo-Jury, F., Schwalm, M., Hamzehpour, L., and Stroh, A. (2020). Brain states govern the spatio-temporal dynamics of resting-state functional connectivity. Elife *9*, e53186.
24. Bukhari, Q., Schroeter, A., and Rudin, M. (2018). Increasing isoflurane dose reduces homotopic correlation and functional segregation of brain networks in mice as revealed by resting-state fMRI. Sci. Rep. *8*, 10591.
25. Casali, A.G., Gosseries, O., Rosanova, M., Boly, M., Sarasso, S., Casali, K.R., Casarotto, S., Bruno, M.A., Laureys, S., Tononi, G., and Massimini, M. (2013). A theoretically based index of consciousness independent of sensory processing and behavior. Sci. Transl. Med. *5*, 198ra105.
26. Sacha, M., Goldman, J.S., Kusch, L., and Destexhe, A. (2024). Asynchronous and Slow-Wave Oscillatory States in Connectome-Based Models of Mouse, Monkey and Human Cerebral Cortex. Appl. Sci. *14*, 1063.
27. Volo, M.D., Romagnoni, A., Capone, C., and Destexhe, A. (2019). Biologically Realistic Mean-Field Models of Conductance-Based Networks of Spiking Neurons with Adaptation. Neural Comput. *31*, 653–680.
28. Gilad, A., and Helmchen, F. (2020). Spatiotemporal refinement of signal flow through association cortex during learning. Nat. Commun. *11*, 1744.
29. Makino, H., Ren, C., Liu, H., Kim, A.N., Kondapaneni, N., Liu, X., Kuzum, D., and Komiyama, T. (2017). Transformation of Cortex-wide Emergent Properties during Motor Learning. Neuron *94*, 880–890.e8.
30. Cole, M.W., Bassett, D.S., Power, J.D., Braver, T.S., and Petersen, S.E. (2014). Intrinsic and task-evoked network architectures of the human brain. Neuron *83*, 238–251.
31. Lynch, L.K., Lu, K.H., Wen, H., Zhang, Y., Saykin, A.J., and Liu, Z. (2018). Task-evoked functional connectivity does not explain functional connectivity differences between rest and task conditions. Hum. Brain Mapp. *39*, 4939–4948.
32. Schroeter, A., Grandjean, J., Schlegel, F., Saab, B.J., and Rudin, M. (2017). Contributions of structural connectivity and cerebrovascular parameters to functional magnetic resonance imaging signals in mice at rest and during sensory paw stimulation. J. Cereb. Blood Flow Metab. *37*, 2368–2382.
33. Wilf, M., Strappini, F., Golan, T., Hahamy, A., Harel, M., and Malach, R. (2017). Spontaneously Emerging Patterns in Human Visual Cortex Reflect Responses to Naturalistic Sensory Stimuli. Cereb. Cortex *27*, 750–763.
34. Krienen, F.M., Yeo, B.T.T., and Buckner, R.L. (2014). Reconfigurable task-dependent functional coupling modes cluster around a core functional architecture. Philos. Trans. R. Soc. Lond. B Biol. Sci. *369*, 20130526.
35. Arfanakis, K., Cordes, D., Haughton, V.M., Moritz, C.H., Quigley, M.A., and Meyerand, M.E. (2000). Combining independent component analysis and correlation analysis to probe interregional connectivity in fMRI task activation datasets. Magn. Reson. Imaging *18*, 921–930.
36. Greicius, M.D., and Menon, V. (2004). Default-mode activity during a passive sensory task: uncoupled from deactivation but impacting activation. J. Cogn. Neurosci. *16*, 1484–1492.
37. Wang, Y., Sibaii, F., Custead, R., Oh, H., and Barlow, S.M. (2020). Functional Connectivity Evoked by Orofacial Tactile Perception of Velocity. Front. Neurosci. *14*, 182.
38. Cirone, D., Pellegrini, F., Cuna, A., Caruso, E., Cimino, L., and Leonardi, F. (2024). Serous macular detachment in ocular toxoplasmosis: A review. Eur. J. Ophthalmol. *34*, 30–38.
39. Mesquita, R.C., Franceschini, M.A., and Boas, D.A. (2010). Resting state functional connectivity of the whole head with near-infrared spectroscopy. Biomed. Opt Express *1*, 324–336.
40. Cabeza, R., Nyberg, L., and Park, D.C. (2017). Cognitive Neuroscience of Aging: Linking

Cognitive and Cerebral Aging (Oxford University Press).
41. Jann, K., Gee, D.G., Kilroy, E., Schwab, S., Smith, R.X., Cannon, T.D., and Wang, D.J.J. (2015). Functional connectivity in BOLD and CBF data: similarity and reliability of resting brain networks. Neuroimage *106*, 111–122.
42. Hendrich, K.S., Kochanek, P.M., Melick, J.A., Schiding, J.K., Statler, K.D., Williams, D.S., Marion, D.W., and Ho, C. (2001). Cerebral perfusion during anesthesia with fentanyl, isoflurane, or pentobarbital in normal rats studied by arterial spin-labeled MRI. Magn. Reson. Med. *46*, 202–206.
43. Drew, P.J., Shih, A.Y., and Kleinfeld, D. (2011). Fluctuating and sensory-induced vasodynamics in rodent cortex extend arteriole capacity. Proc. Natl. Acad. Sci. USA *108*, 8473–8478.
44. Manahan-Vaughan, D. (2018). Handbook of in Vivo Neural Plasticity Techniques: A Systems Neuroscience Approach to the Neural Basis of Memory and Cognition (Academic Press).
45. Sullender, C.T., Richards, L.M., He, F., Luan, L., and Dunn, A.K. (2022). Dynamics of isoflurane-induced vasodilation and blood flow of cerebral vasculature revealed by multi-exposure speckle imaging. J. Neurosci. Methods *366*, 109434.
46. Xie, H., Chung, D.Y., Kura, S., Sugimoto, K., Aykan, S.A., Wu, Y., Sakadžić, S., Yaseen, M.A., Boas, D.A., and Ayata, C. (2020). Differential effects of anesthetics on resting state functional connectivity in the mouse. J. Cereb. Blood Flow Metab. *40*, 875–884.
47. Massimini, M., Ferrarelli, F., Huber, R., Esser, S.K., Singh, H., and Tononi, G. (2005). Breakdown of cortical effective connectivity during sleep. Science *309*, 2228–2232.
48. Goldman, J.S., Kusch, L., Aquilue, D., Yalçınkaya, B.H., Depannemaecker, D., Ancourt, K., Nghiem, T.A.E., Jirsa, V., and Destexhe, A. (2022). A comprehensive neural simulation of slow-wave sleep and highly responsive wakefulness dynamics. Front. Comput. Neurosci. *16*, 1058957.
49. Goldman, S.J., Kusch, L., Yalcinkaya, H.B., Depannemaecker, D., Nghiem, T.E., Jirsa, V., and Destexhe, A. (2020). Brain-scale emergence of slow-wave synchrony and highly responsive asynchronous states based on biologically realistic population models simulated in The Virtual Brain. Preprint at bioRxiv. https://doi.org/10.1101/2020.12.28.424574.
50. Frohlich, J., Bayne, T., Crone, J.S., DallaVecchia, A., Kirkeby-Hinrup, A., Mediano, P.A.M., Moser, J., Talar, K., Gharabaghi, A., and Preissl, H. (2023). Not with a 'zap' but with a 'beep': Measuring the origins of perinatal experience. Neuroimage *273*, 120057.
51. Shahsavarani, S., Thibodeaux, D.N., Xu, W., Kim, S.H., Lodgher, F., Nwokeabia, C., Cambareri, M., Yagielski, A.J., Zhao, H.T., Handwerker, D.A., et al. (2023). Cortex-wide neural dynamics predict behavioral states and provide a neural basis for resting-state dynamic functional connectivity. Cell Rep. *42*, 112527.
52. Marguet, S.L., and Harris, K.D. (2011). State-dependent representation of amplitude-modulated noise stimuli in rat auditory cortex. J. Neurosci. *31*, 6414–6420.
53. Schölvinck, M.L., Saleem, A.B., Benucci, A., Harris, K.D., and Carandini, M. (2015). Cortical state determines global variability and correlations in visual cortex. J. Neurosci. *35*, 170–178.
54. Curto, C., Sakata, S., Marguet, S., Itskov, V., and Harris, K.D. (2009). A simple model of cortical dynamics explains variability and state dependence of sensory responses in urethane-anesthetized auditory cortex. J. Neurosci. *29*, 10600–10612.
55. Manita, S., Suzuki, T., Homma, C., Matsumoto, T., Odagawa, M., Yamada, K., Ota, K., Matsubara, C., Inutsuka, A., Sato, M., et al. (2015). A Top-Down Cortical Circuit for Accurate Sensory Perception. Neuron *86*, 1304–1316.
56. Yamashita, T., and Petersen, C.C. (2016). Target-specific membrane potential dynamics of neocortical projection neurons during goal-directed behavior. Elife *5*, e15798.
57. Kwon, S.E., Yang, H., Minamisawa, G., and O'Connor, D.H. (2016). Sensory and decision-related activity propagate in a cortical feedback loop during touch perception. Nat. Neurosci. *19*, 1243–1249.
58. Romo, R., and Rossi-Pool, R. (2020). Turning Touch into Perception. Neuron *105*, 16–33.
59. Nietz, A.K., Popa, L.S., Streng, M.L., Carter, R.E., Kodandaramaiah, S.B., and Ebner, T.J. (2022). Wide-Field Calcium Imaging of Neuronal Network Dynamics In Vivo. Biology (Basel) *11*, 1601.
60. Harris, J.A., Mihalas, S., Hirokawa, K.E., Whitesell, J.D., Choi, H., Bernard, A., Bohn, P., Caldejon, S., Casal, L., Cho, A., et al. (2019). Hierarchical organization of cortical and thalamic connectivity. Nature *575*, 195–202.
61. Chen, T.W., Wardill, T.J., Sun, Y., Pulver, S.R., Renninger, S.L., Baohan, A., Schreiter, E.R., Kerr, R.A., Orger, M.B., Jayaraman, V., et al. (2013). Ultrasensitive fluorescent proteins for imaging neuronal activity. Nature *499*, 295–300.
62. Dana, H., Mohar, B., Sun, Y., Narayan, S., Gordus, A., Hasseman, J.P., Tsegaye, G., Holt, G.T., Hu, A., Walpita, D., et al. (2016). Sensitive red protein calcium indicators for imaging neural activity. Elife *5*, e12727.
63. Russell, L.E., Fişek, M., Yang, Z., Tan, L.P., Packer, A.M., Dalgleish, H.W.P., Chettih, S.N., Harvey, C.D., and Häusser, M. (2024). The influence of cortical activity on perception depends on behavioral state and sensory context. Nat. Commun. *15*, 2456.
64. Lee, C.C.Y., Kheradpezhouh, E., Diamond, M.E., and Arabzadeh, E. (2020). State-Dependent Changes in Perception and Coding in the Mouse Somatosensory Cortex. Cell Rep. *32*, 108197.
65. Conti, E., Allegra, M.A.L., and Pavone, F.S. (2019). Large Scale Double-Path Illumination System with Split Field of View for the All-Optical Study of Inter-and Intra-Hemispheric Functional Connectivity on Mice. Methods Protoc *2*, 11.
66. Quarta, E., Scaglione, A., Lucchesi, J., Sacconi, L., Allegra Mascaro, A.L., and Pavone, F.S. (2022). Distributed and Localized Dynamics Emerge in the Mouse Neocortex during Reach-to-Grasp Behavior. J. Neurosci. *42*, 777–788.
67. Allegra, M.A.L., Falotico, E., Petkoski, S., Pasquini, M., Vannucci, L., Tort-Colet, N., Conti, E., Resta, F., Spalletti, C., Ramalingasetty, S.T., et al. (2020). Experimental and Computational Study on Motor Control and Recovery After Stroke: Toward a Constructive Loop Between Experimental and Virtual Embodied Neuroscience. Front. Syst. Neurosci. *14*, 31.
68. Tort-Colet, N., Resta, F., Montagni, E., Pavone, F., Allegra Mascaro, A.L., and Destexhe, A. (2023). Assessing brain state and anesthesia level with two-photon calcium signals. Sci. Rep. *13*, 3183.
69. Scott, B.B., Thiberge, S.Y., Guo, C., Tervo, D.G.R., Brody, C.D., Karpova, A.Y., and Tank, D.W. (2018). Imaging Cortical Dynamics in GCaMP Transgenic Rats with a Head-Mounted Widefield Macroscope. Neuron *100*, 1045–1058.e5.
70. Esmaeili, V., Tamura, K., Muscinelli, S.P., Modirshanechi, A., Boscaglia, M., Lee, A.B., Oryshchuk, A., Foustoukos, G., Liu, Y., Crochet, S., et al. (2021). Rapid suppression and sustained activation of distinct cortical regions for a delayed sensory-triggered motor response. Neuron *109*, 2183–2201.e9.

STAR★METHODS

KEY RESOURCES TABLE

REAGENT or RESOURCE	SOURCE	IDENTIFIER
Experimental models: Organisms/strains		
Mouse: C57BL/6J-Tg(Thy1-GCaMP6f)GP5.17Dkim/J	The Jackson Laboratory	Strain #:025393; RRID: IMSR_JAX:025393
Software and algorithms		
OriginPro	OriginLab	https://www.originlab.com/
Python	Python	https://www.python.org/
Matlab2019	Matlab	https://mathworks.com/
ImageJ	Fiji	https://imagej.net/

RESOURCE AVAILABILITY

Lead contact

Requests for further information should be addressed to the lead contact or the correspondence author (allegra@lens.unifi.it; montagni@lens.unifi.it).

Materials availability

This study did not generate new unique reagents.

Data and code availability

- The data in the main figures and tables that support the findings of this study are available from the corresponding author upon request.
- The codes used in this study for analyzing calcium imaging data are available from the corresponding author upon request.
- Any additional information required to reanalyze the data reported in this paper is available from the corresponding author upon request.

EXPERIMENTAL MODEL AND STUDY PARTICIPANT DETAILS

All experiments were performed in accordance with the guidelines of the Italian Minister of Health (aut. n. 857/2021). A total of 9 mice (6-12 months), C57BL/6J-Tg(Thy1-GCaMP6f)GP5.17Dkim/J, Strain #:025393, RRID:IMSR_JAX:025393 heterozygous of both sexes were used.

METHOD DETAILS

Intact-skull preparation

Mice were anesthetized with isoflurane (3% for induction, 1–2% for maintenance) and placed in a stereotaxic apparatus (KOPF, model 1900). Ophthalmic gel (Lacrilube) was applied to prevent eye drying, body temperature was maintained at 36°C using a heating pad and lidocaine 2% was used as local anaesthetic. The skin and the periosteum were cleaned and removed. Bregma was signed with a black fine-tip pen. A custom-made aluminium head-bar placed behind lambda and the exposed skull were sealed using transparent dental cement (Super Bond C&B – Sun Medical). After the surgery, mice were recovered in a temperature- and humidity-controlled room, with food and water *ad libitum* for two weeks before recordings.

Imaging setup

The wide-field imaging setup was slightly modified from.[65,66] Wide-field calcium imaging was performed through the intact skull using a custom-made microscope. The excitation source for GCaMP6f was a blue-light beam of emitting diode (470nm LED light, M470L3 Thorlabs, New Jersey, United State). The excitation band was selected by a bandpass filter (482/18 Semrock, Rochester, New York, NY, USA). The light beam was deflected by a dichroic mirror (DC FF 495-DI02 Semrock, Rochester, New York, NY, USA) on the objective (TL2X-SAP 2 Super Apochromatic Microscope Objective, 0.1 NA, 56.3 mm WD).

Reflectance images were acquired using a light source positioned at 45° incident to the brain surface (530 nm LED light, M530L4; Thorlabs, New Jersey, United State). The excitation band was selected by a bandpass filter (525/50 nm filter). Both the fluorescence signal and the reflectance changes were collected through a band-pass filter (525/50, Semrock, Rochester, New York, USA) and collected by a high-speed complementary metal-oxide semiconductor (CMOS) camera (ORCA-Flash4.0 V3 Digital CMOS camera / C13440-20CU, Hamamatsu).

Reflectance data are acquired interlaced with fluorescence data by using a camera configured to acquire images in synchrony with two strobing LEDs (sampling rate: 40Hz per LED). To rule out the possibility of auditory responses from environmental sounds (e.g., picospritzer), white noise at 80 dB was delivered through stereo speakers positioned on both sides of the microscope stage.

Awake imaging

After the post-surgical recovery period (3 days), mice (n = 5) were acclimatized to the head-fixation for two consecutive days (15 min a day/mouse). This was followed by 50-60 minutes of imaging session in which both spontaneous (38 s-long, 5 repetitions) and perturbed activity (24 s-long, 30 repetitions) were recorded.

Anesthetized imaging

Days following awake imaging, mice were anesthetized by isoflurane to investigate three brain states.

According to the literature, we modulated isoflurane concentration to stabilize global rhythmic activity (averaged across the entire field of view) at approximately 0.1-0.2 Hz for the "deep" anesthesia level (Dasilva et al., 2021). Slight adjustments to the isoflurane concentration resulted in global activity exhibiting higher upstate frequencies of 0.2-0.4 Hz, categorizing recordings in this state as a medium anesthesia level. The light anesthesia level was achieved at a low isoflurane concentration, wherein the global rhythmic activity displayed long-lasting up-states spaced out by short down-states. The average isoflurane concentrations were 1.71 $\pm$ 0.08 %, n = 6 in DEEP anesthesia, 1.49 $\pm$ 0.06 %, n = 6 in MEDIUM anesthesia and 1.32 $\pm$ 0.12 %, n = 5 in LIGHT anesthesia. Potential discrepancies in isoflurane concentrations may arise due to our exclusive use of isoflurane as an anaesthetic, in contrast to other studies.[12]

Each anesthesia level was maintained for 60 minutes, and recordings were consistently monitored to conserve a stable slow-oscillatory regime. Spontaneous activity recordings (38 s-long, 5 repetitions) and perturbed activity recordings (24 s-long, 30 repetitions) were acquired in the same daily session per brain state. Due to the instability of anaesthesia after a few hours, deep and medium anesthesia were recorded consecutively on the same imaging session per mouse, starting from the higher isoflurane concentration to the lower. Light anesthesia was instead recorded on a subsequent day as it requires more time to be stabilized. During the whole anesthetic treatment, body temperature was maintained at 37°C by a feedback-controlled thermostatic heating pad.

Whisker stimulation

Stimulation was delivered to the left whiskers through a tubing system using an electrically gated pressure injector (Picospritzer III—Science Products). Whiskers were deflected ~1 cm in the rostrocaudal direction. A single stimulation trial consisted of 24 s designed as 13 s rest, 1 s of stimulation with a blowing time of 60 ms, and 10 s rest. Each experiment session consisted of 30 trials per animal (n = 9 mice).

Computational model

Simulations of awake and anesthetized brain states were obtained in The Virtual Brain (TVB) with a mouse version of the TVB-AdEx model,[48] parcellated according to the Allen Brain mouse atlas into 512 nodes or cortical regions. In each node we modeled a mean field network of excitatory and inhibitory AdEx neurons. As in Goldman et al., 2023,[48] in order to switch the whole brain network dynamics from asynchronous irregular (awake-like) to the synchronous oscillatory regime (characteristic from unconscious states such as sleep or anesthesia) we varied the strength of spike-frequency adaptation of the excitatory population of each node (parameter b in the figures). Firing rates were converted to calcium imaging signals through implementing a calcium monitor to the TVB model as in.[67,68] We simulated evoked responses in each brain state by applying an input current of 60 ms to the right barrel field cortex node. The onset of the stimulus was randomly delayed in each trial.

Data analysis

Images were recorded at a frame rate of 40Hz per LED, with a resolution of 512 x 512 pixels and a FOV of ~ 12 x 12 mm (depth 16-bit) via custom-made software. All data analyses were performed in MATLAB (MathWorks), Phyton, ImageJ, and Origin.

For each pixel, hemodynamic correction was performed as described by.[69] Briefly, using the ratiometric approach:

$$\frac{F}{F_o} = \frac{\frac{I^{482}}{I_0^{482}}}{\frac{I^{525}}{I_0^{525}}}$$

Where F/F_0 is the final corrected GCaMP6 time series for a given pixel, I^{482} refers to the detected fluorescence signal, I^{525} is the reflectance signal. I was the intensity value of that pixel in a specific time point and I0 was the mean fluorescence intensity of the signal averaged across the whole time window (for the spontaneous activity) or across the pre-stimulus window (for perturbed activity).

To dissect the contribution of each cortical area for both awake and anesthetized activity, the plane of imaging was projected to the surface of the Allen Institute Mouse Brain Atlas (www.brain-map.org) as described by.[28,66,70] Briefly, bregma-lambda alignment was based on stereotaxic coordinates and subsequently confirmed using the early responsiveness area activated by whisker stimulation in the awake state. Next, on the following experimental sessions, we were able to precisely position the head using the lambda and bregma coordinates for the same animal.

A mask was applied to exclude areas laying on the most lateral parts of the mouse cortex and the fluorescence time course was measured by averaging all pixels within individual areas. The neocortex parcellation created 17 areas for each hemisphere, for a total of 34 areas. The abbreviations and extended names for each area are as follows: MOs, secondary motor area; MOp, primary motor area; SSp-bfd, primary somatosensory area, barrel field; SSp-ll, primary somatosensory area, lower limb; SSp-m, primary somatosensory area, mouth; SSp-n, primary somatosensory area, nose; SSp-tr, primary somatosensory area, trunk; SSp-ul, primary somatosensory area, upper limb; SSp-un, primary somatosensory area, unassigned; RSPagl, retrosplenial area, lateral agranular part; RSPd, retrosplenial area, dorsal part; VISrl, rostrolateral visual area; VISa, anterior visual area; VISal, anterolateral visual area; VISam, anteromedial visual area; VISp, primary visual area; and VISpm, posteromedial visual area. The suffixes L and R were added to refer to the left (ipsilateral with respect to the whisker stimulation) or right hemisphere (contralateral with respect to the whisker stimulation) (e.g., MOp_L, MOp_R).

To quantify the durations of the up states, the calcium signal had to exceed a critical threshold defined by 2 SD the lowest mean activity computed across the entire cortex. Then, the time between two up states was used as down state duration. To avoid random oscillation detection, both the up and down state durations were set to a minimum of 75ms. This threshold was heuristically set after a visual inspection of the signal. Individual perturbed activity trials were discarded prior to analysis if there was an ongoing up state at the time of stimulation in anesthesia.

Functional connectivity and network analyses

Three different types of connectivity analyses were performed to assess the impact of the brain state on the FC in both spontaneous and perturbed activity: global, inter- and intra-hemispheric connectivity analysis, and area pair-wise analysis. These analyses were carried out on 2-sec post-stimulus windows for perturbed activity and on 30 randomly selected 2-sec windows for spontaneous activity. Functional connectivity was calculated as the Pearson's correlation coefficient between signal time series of various cortical regions at the single-trial level. Connectivity scores were averaged over trials within conditions, but independently for each mouse. These scores were subsequently averaged across mice within each brain state. In order to visualize the matrix of differences, the average FC scores of one brain state were subtracted from the corresponding average FC scores of another brain state. To enable parametric statistical testing, correlation coefficients were additionally Fisher z-transformed.

Right and left intra-hemispheric FC were quantified by averaging correlation values within all right and left-hemisphere cortical regions, respectively. Inter-hemispheric FC was measured by averaging correlation values between all right- and left-hemisphere region pairs. By averaging every combination value previously obtained, global FC was calculated. Intra/inter FC ratio was performed by dividing the two average values per mouse. For area pair-wise analysis multiple comparisons were corrected by Benjamini–Hochberg procedure. The significance of the correlation analysis was set at a threshold of (Benjamini–Hochberg) corrected $P < 0.05$.

No statistical methods were used to predetermine the sample size.

Quantitative analysis of perturbed activity

Before processing, the calcium response evoked by stimulation was averaged across 30 trials per cortical area per mouse and per brain state. The onset of the response was defined as the time when the signal crosses a threshold corresponding to the averaged baseline amplitude (1 s before the start of the stimulus) + 2 SD. Only trials with post-stimulus amplitude higher than the threshold in a 2-second window were included in the analysis.

The parameter "time to peak" was quantified as the time interval (s) between the stimulus pulse and the peak response. The response duration was the time interval between the onset of the response and the point at which the activity decreased under the previously determined threshold in a 2-second window. Then, the maximum response was calculated at the time to peak and the FWHM (full width for half-maximal amplitudes) was the interval between time points for half-maximal amplitudes at the ascending and the descending arm of a peak. The rise and decay slope were calculated by a least-squares fit to the trace during the transient.

For only deep and medium anesthesia a single trial analysis was performed to quantify the first and second peak at a single stimulus level and then the analyzed data were averaged across trials per animal. Before processing, single activity traces were temporally smoothed to improve SNR. Six principal areas per hemisphere were selected: MOs, secondary motor area; MOp, primary motor area; SSp-bfd, primary somatosensory area, barrel field; SSp-tr, primary somatosensory area, trunk; VISp, primary visual area; and RSPd, retrosplenial area, dorsal part. The suffixes L and R were added to refer to the left (ipsilateral with respect to the whisker stimulation) or right hemisphere (contralateral with respect to the whisker stimulation) (eg., MOp_L, MOp_R). Only the fraction of trials detected as responsive for the first peak were used to calculate the probability of the second peak.

CI analysis

The Complexity Index (CI) was computed in response to an external stimulus in line with the method proposed by.[25] The CI is the ratio of two quantities: the Lempel-Ziv algorithmic complexity and the source entropy. To compute both quantities, the calcium signal intensity was calculated and binarized to produce significance vectors s(t). Different trials of the same stimulus were aligned to stimulation time, considering the 600 ms before and after stimulus onset/offset. Then, each node over the hemisphere is re-scaled by mean and standard deviation given by pre-stimulus activity, averaged over nodes. After all pre-stimulus signals are randomized across time bins, this procedure is repeated 500 times. The threshold for significance T is then given by the one-tail percentile of the maximum absolute value over all repetitions within a series of 20 trials. For each trial of those 20 trials, we can then write $s(t) = 1$ whenever post-stimulus calcium signal $C(t) > T$ and $S(t) = 0$ otherwise.

The Lempel-Ziv complexity LZ(S) is the length of the 'zipped' vector S(t), i.e. the number of possible binary 'words' that make up the binary vector S(t). Briefly, S(t) is sectioned successively into consecutive words of between one and N_t characters where N_t is the total length of S(t). Scanning sequentially through all words, each newly encountered word is added to a 'dictionary', and LZ(S) is the total number of words in the dictionary at the end of the procedure.

The spatial source entropy H(S) is given by:

$$H(S) = -p(S=0)log_2(p(S=0)) - p(S=1)log_2(p(S=1))$$

where $\log_2$ denotes the base-two logarithm.

The CI can then be expressed as,

$$CI(S) = \frac{LZ(S)}{H(S)}$$

In the model, the CI was calculated analogously to experimental data, taking as signal the calcium signal generated by the TVB model in each region. Thus, the nodes were given by the different cortical regions of the TVB model.

QUANTIFICATION AND STATISTICAL ANALYSIS

All statistical analysis was performed in OriginLab (2019) and R. Data are shown as mean $\pm$ s.e.m. For multiple comparisons across four brain states (awake, light, medium and deep) linear mixed-effect model (MLE) was used defining the animals as a random factor. For the single-trial analysis two-way ANOVA was used and Bonferroni correction was applied for post-hoc t-tests. For the CI analysis, since the model can simulate the activity for each brain state and cannot account for the inter-animal variability, we applied the Kruskal-Wallis test and post-hoc Dunn's test with Bonferroni correction. In the figures, significance levels are represented with the following convention: * for $p<0.05$; ** for $p<0.01$, *** for $p<0.001$.